DESIGN OF AUTOMOTIVE TRACTION POWER DISTRIBUTION CONTROLLER CONSIDERING THE ABS ACTUATOR

Phan Tan Tai[1], Tran Van Nhu[2]*, Ngo Thanh Ha[1], Phan Van Tuan[1]

[1]*Tra Vinh University, Vietnam*

[2]*University of Transport and Communications, Vietnam*

*Corresponding author: vannhu.tran@utc.edu.vn

(Received: March 28, 2025; Revised: October 21, 2025; Accepted: December 10, 2025)

DOI: 10.31130/ud-jst.2025.23(12).169

Abstract - The contact state between the wheel and the road surface significantly affects automotive traction performance. On rough roads, differential slippage between the left and right wheels leads to uneven traction power, which may cause vehicle instability or immobilization, resulting in engine power loss. This study proposes a method for managing traction power by controlling the ABS actuator to generate wheel slip resistance as required. In this paper, a cascade controller is developed to regulate both the speed of the drive wheels and the oil pressure in the wheel brake mechanism, thereby preventing wheel slip. This approach enables the differential to distribute power more effectively to the active axle, enhancing engine efficiency. System evaluation using Matlab/Simulink software demonstrate the high responsiveness of the proposed solution.

Keywords - traction control; cascade controller; ABS actuator; brake control

1. Introduction

Controlling the traction power at the drive axle wheels is intended to enhance engine power utilization efficiency and improve the road-holding capability of automotive drive wheels. Recent challenges include determining wheel adhesion states, monitoring slip process to control and reduce slippage, maintaining wheel slip within permissible limits, and employing nonlinear predictive control strategies to achieve optimal slip speed [1-2]. Some studies utilize tire friction models, such as Pacejka or Dugoff, to estimate tire slip for traction control [3-4]. Additionally, various control methods have been developed to regulate wheel braking force, thereby increasing the resistive torque for slipping wheels to facilitate appropriate traction power distribution [5-6] or by combining brake resistance control with engine torque control [7]. These approaches primarily target optimal wheel slip ratio. However, the slip ratio is difficult to measure or estimate accurately, so most research has concentrated on calculation and simulation, often neglecting the influence of power transmission paths in the differential.

The Anti-lock Braking System (ABS) is considered a significant contribution to traffic safety, as it is designed to maintain stability during emergency braking and prevent wheel lock-up. Wheels tend to slip and lock up when subjected to sudden braking or when braking on slippery surfaces, resulting in extended stopping distances and, at times, loss of vehicle stability. The integration of ABS enables vehicles to stop within the shortest possible distance while maintaining steering control. Over the years, numerous ABS technologies have been applied to traction control and vehicle dynamic stability control systems [8-10]. Control systems based on engine output torque to the drive wheels have been designed [11-12], wherein engine torque is regulated to achieve traction control objectives through throttle valve control or driver pedal input [10]. Other studies have utilized braking torque at the wheel brake mechanism to control power transmission from the engine output shaft to the driven half-shafts via the ABS actuator [8], [13-14], in order to manage wheel slip speed during acceleration on slippery roads or to efficiently transmit traction torque to the drive wheels [15-17]. The research on "Calculation and Simulation of Hydraulic ABS Controller" by Cai Jian-Wei and colleagues [18] established models such as the oil pump, intake/exhaust valves, electric motor, and accumulator. Experimental results from this work revealed the relationship between changes in hydraulic oil pressure and the orifice area of the intake and exhaust valves in the actuator, thereby evaluating the responsiveness of the hydraulic controller during ABS operation in vehicles.

Based on the aforementioned studies, the content of this paper focuses on the design of a cascade controller for automotive traction power control, taking into account the hydraulic ABS actuator. This controller manages the speed of the wheels on the drive axle and regulates the brake oil pressure to create resistance at slipping wheels, thereby enabling more uniform transmission of traction power among the wheels on the drive axle and improving the efficiency of engine power utilization. Specific survey results are evaluated in detail to demonstrate the high effectiveness of the designed controller.

2. Methodology for designing the automotive traction power control system considering the ABS actuator

2.1. Development of the traction power control model

A Proportional-Integral-Derivative (PID) controller is employed to regulate the distribution of traction power at the wheels on the drive axle. Based on the drivetrain dynamics model and assumptions from previous studies [16-17], the resulting models - engine, power transmission system, and vehicle motion - are represented by Equation 1, where: J_e, J_h, J_{tr}, J_{ph} denotes the moment of inertia of the rotating components of the engine, gearbox, left and right wheels; $\ddot{\theta}_e, \ddot{\theta}_h, \ddot{\theta}_3, \ddot{\theta}_4, \ddot{\theta}_{tr}, \ddot{\theta}_{ph}$ represents the angular acceleration of the engine output shaft, gearbox, left and right half-shafts, left and right wheels; $F_\omega, F_f, F_{tr}, F_{ph}$ are the aerodynamic

drag, rolling resistance, and traction forces at the left and right wheels on the drive axle, respectively; $M_e, M_h, M_0, M_3, M_4, M_{f21}, M_{f22}$ sequentially represent the output torque at the engine, gearbox, main drive shaft, left and right half-shafts, and the resistive torque at the left and right half-shaft gears.

To ensure efficient power distribution by the differential to the wheels on the drive axle, it is necessary to calculate the wheel slip in order to control their speeds to be equal. In cases where the vehicle is stuck, one wheel may be spinning freely while the other remains stationary on a good road surface, preventing the vehicle from moving and resulting in engine power loss due to poor tire-road adhesion. The PID controller is designed to generate a resistive force (brake torque) at the brake mechanism of the slipping wheel, helping to equalize the rotational speeds of the drive axle wheels [16]. Thus, engine output power is utilized more efficiently, and the differential distributes power more evenly between the two wheels. Figure 1 illustrates the PID controller design diagram, where: ω_{tr}, ω_{ph} are the rotational speeds of the left and right wheels, respectively; e is the speed deviation of the drive axle wheels; u_p is the brake torque signal applied to the brake mechanism as required.

$$\begin{cases} \ddot{\theta}_e=(M_e-M_h)/J_e \\ \ddot{\theta}_h=(M_h-M_0)/J_h \\ \ddot{\theta}_3=[A(M_0\frac{i_0}{2}-M_3)-B(M_0\frac{i_0}{2}-M_4)]/(A^2-B^2) \\ \ddot{\theta}_4=[B(M_0\frac{i_0}{2}-M_3)-A(M_0\frac{i_0}{2}-M_4)]/(B^2-A^2) \\ \ddot{\theta}_{tr}=(M_3-F_{tr}r_{bx}-M_{f21})/J_{tr} \\ \ddot{\theta}_{ph}=(M_4-F_{ph}r_{bx}-M_{f22})/J_{ph} \\ m\ddot{x}=F_{tr}+F_{ph}-F_\omega-F_f \end{cases} \quad (1)$$

With $\begin{cases} A=J_0\frac{i_0^2}{4}+\frac{J_1}{4}+J_3+2J_2i_2^2 \\ B=J_0\frac{i_0^2}{4}+\frac{J_1}{4}-2J_2i_2^2 \end{cases}$

The input signal is the speed deviation e, and the output signal is sent to the brake actuator to control the brake mechanism, generating a large brake torque at the slipping wheel. Assuming that the left wheel is rolling on a slippery surface, when a speed deviation occurs $(e>0)$, the PID controller outputs a brake torque signal (M_{pd}) to brake the left wheel, reducing its angular velocity and consequently decreasing the deviation to zero $(e\to 0)$. This control model is described by Equation 2, where: $e(t)=\left[\omega_{tr}-\omega_{ph}\right]_0^t$; K_p, K_i, K_d are the weights of the error, integral, and derivative components, respectively.

$$M_{pd}=K_pe(t)+K_i\int_0^t e(\tau)d\tau+K_d\dot{e}(t) \quad (2)$$

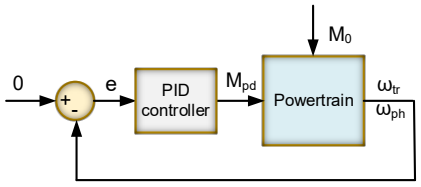

Figure 1. *Brake torque control model*

2.2. Development of the ABS actuator dynamics model

The dynamics model of the brake actuator describes the relationship between the solenoid valves, hydraulic flow in the circuit, and the braking process at the wheel. The schematic diagram of the valves and hydraulic cylinder at the wheel is shown in Figure 2, where: Q_s, Q_v are the oil flow rates into and out of the intake valve; Q_c, Q_t are the oil flow rates into (oil supplied to the wheel cylinder) and out of the exhaust valve; p_s, p_t are the oil pressures at the intake valve inlet and outlet; p_c is the oil pressure supplied to the wheel cylinder; m_p is the mass of the wheel brake cylinder piston; V_0 is the initial volume in the wheel brake cylinder; x_0 is the initial distance between the two pistons in the wheel brake cylinder; x_p is the displacement of the piston in the wheel brake cylinder; C_b is the viscous damping coefficient of the piston and brake pad movement; K_b is the equivalent stiffness of the brake pad and return spring.

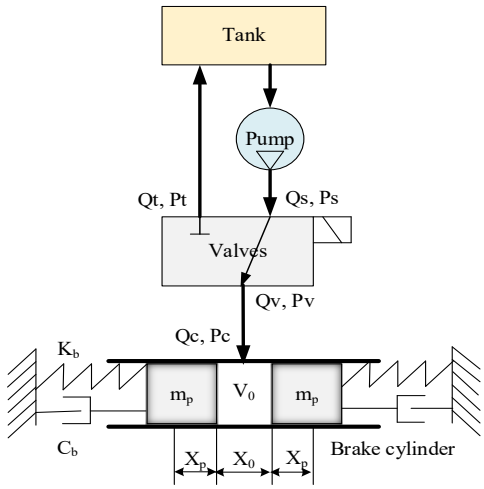

Figure 2. *The overall hydraulic circuit schematic of a wheel brake cylinder part*

2.2.1. Dynamics model of hydraulic valves

The intake and exhaust valves are typically solenoid-type, functioning as high-speed switches. When a voltage pulse from the brake torque controller is applied, the valve operates. Equation 3 calculates the displacement velocity of the valves in the actuator [19], where: U is the solenoid valve opening voltage; U_0 is the high voltage level of the pulse; x_{0v} is the maximum stroke of the valve needle;

x_v is the displacement of the valve needle; τ is the time constant.

$$\dot{x}_v = \frac{1}{\tau x_{0v}} x_v + \frac{U}{\tau U_0} \tag{3}$$

The system operates by supplying oil flow at a certain pressure from the pump, with the oil pressure through the pump considered stable throughout system operation. Equation 4 determines the oil flow through the intake and exhaust valves when open [20], where: C_d is the flow coefficient, ρ is the density of brake oil, and A_f, A_d is the orifice area of the intake and exhaust valves.

$$\begin{cases} Q_s = C_d A_f \sqrt{\dfrac{2|p_s - p_v|}{\rho}} sign(p_s - p_v) \\ Q_t = C_d A_d \sqrt{\dfrac{2|p_c - p_t|}{\rho}} sign(p_c - p_t) \end{cases} \tag{4}$$

The orifice area of the intake and exhaust valves during operation is determined by two states: closed and open. Equation 5 calculates the orifice area value of the intake and exhaust valves, where: A_{of}, A_{od} is the fully open orifice area of the intake and exhaust valves.

$$\begin{cases} A_f = \begin{cases} A_{of} \rightarrow (x_v > 0) \\ 0 \rightarrow (x_v = 0) \end{cases} \\ A_d = \begin{cases} A_{od} \rightarrow (x_v > 0) \\ 0 \rightarrow (x_v = 0) \end{cases} \end{cases} \tag{5}$$

2.2.2. Dynamics model of the hydraulic circuit

From Figure 2, the oil flow in the hydraulic circuit from the intake valve to the exhaust valve can be determined using Equation 6.

$$Q_v = Q_s - Q_t \tag{6}$$

Assuming the pressure at the intake valve outlet and the pressure at the wheel cylinder are equal, the pressure dynamics equation is calculated by Equation 7, where: β is the bulk modulus of the oil, and A_p is the cross-sectional area of the piston in the wheel brake cylinder.

$$\dot{p}_v = \dot{p}_c = \frac{\beta}{V_0 + 2x_p A_p} (Q_v - 2\dot{x}_p A_p) \tag{7}$$

2.2.3. Dynamics model of the wheel brake mechanism

Drum brakes are selected for this brake mechanism, and the dynamics equation is described by Expression 8, where: M_p is the brake torque generated at the wheel; K is the structural coefficient of the brake mechanism at the wheel. $K = \dfrac{M_{p\max}}{p_{c\max} - p_t}$.

$$\begin{cases} \ddot{x}_p = \dfrac{1}{m_p}(p_c A_p - x_p K_b - \dot{x}_p C_b) \\ M_p = K(p_c - p_t) \end{cases} \tag{8}$$

2.3. Design of the traction power control system considering the brake actuator

The traction power control system is designed with two control layers, also known as a cascade controller. There are two component controllers (Figure 3): the outer loop controller (Controller A) calculates the required brake torque for wheel braking (M_{pd}); the inner loop controller (Controller B) controls the brake oil pressure (p_c) in the wheel brake cylinder to ensure that the generated brake torque (M_p) matches the required brake torque calculated by Controller A. If there is a deviation in brake pressure (e_p), it outputs a voltage signal U_s or U_d to the ABS actuator, activating the intake and exhaust valves to ensure that M_p reaches the desired value.

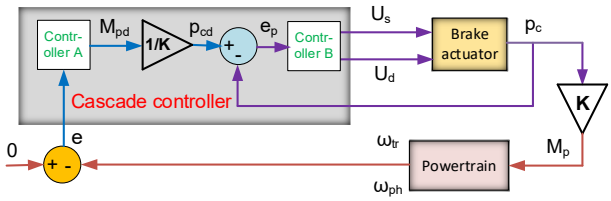

Figure 3. *Schematic diagram of the cascade controller*

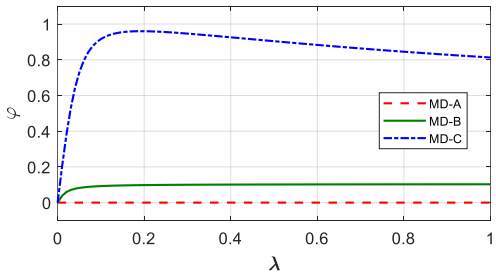

Figure 4. *Relationship between adhesion and slip coefficient on surveyed road types*

The traction power control system is surveyed using Matlab/Simulink software with the cascade controller in the scenario where the vehicle travels straight on a non-uniform road, with the right wheel moving on a good road surface (MD-C) and the left wheel rolling on a poor adhesion surface (MD-B) or a slippery surface (MD-A). Figure 4 illustrates the relationship between slip ratio and adhesion on the three surveyed road types, where: MD-C is a road with good adhesion $(\varphi = 0.8 \div 1)$, with a slip ratio about $(\lambda = 20\%)$; MD-B is a road with low adhesion $(\varphi \approx 0.1)$, with minimal wheel spin; MD-A is a road with very low adhesion $(\varphi = 0.001)$, with a slippery surface, with the wheel spinning freely $(\lambda = 100\%)$. When the vehicle travels on MD-C, the drive axle wheel speeds are nearly equal, and this case is not considered as the controller is inactive. Therefore, subsequent sections will only present survey results for MD-A and MD-B road types.

3. Results and discussion

The traction power distribution control model for the vehicle axle was investigated using Matlab/Simulink

software. Manual tuning was applied, and the selected control parameters were set as follows: $K_p = 500, K_i = 10, K_d = 0.1$. The survey results indicate that the traction power distributed by the differential to the drive axle varies depending on the slip state of the wheels relative to the road surface. The power distribution process is illustrated in Figure 5, where: $N_e, N_k, N_{tt}, N_{tp}, N_{tr}, N_{ph}$ denote the engine power, total traction power, power at the half-shafts, and at the left and right wheels, respectively. In the case where the left wheel rolls on MD-A, the engine power transmitted to both half-shafts is approximately equal, each about 50% of the engine power. However, the power at the left wheel is very low, nearly zero, due to complete slippage (Figure 5a), while the power at the right wheel equals the total traction power. This allows the vehicle to pass through slippery regions more easily, avoiding engine power waste. In the case where the left wheel rolls on MD-B, with less slippage, the power at the left wheel increases, raising the total traction power to 62.23% of the engine power (Figure 5b).

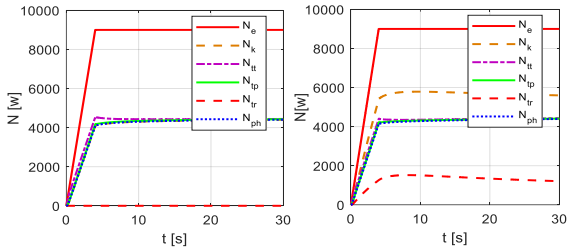

a/ MD-A *b/ MD-B*

Figure 5. *Traction power is distributed on both sides of the driving wheels*

Although the power at both half-shafts equals the total traction power $(N_{tt} = N_{tp} = N_k)$, complete slippage of the left wheel causes the traction torque at the left wheel to be zero (Figure 6b). A similar survey on MD-B shows that the traction torque at the left wheel increases significantly as slip decreases. Without the controller, when the left side of the vehicle boggs down $(\lambda = 1)$, the wheel speed rapidly increases, while the right wheel remains stationary, resulting in the vehicle being unable to move. When the cascade controller is used, Controller A sends a brake torque signal to Controller B, which commands the ABS actuator to generate brake torque at the left wheel, gradually reducing its rotational speed to match that of the right wheel $(\omega_{tr} = \omega_{ph})$ (Figure 6a), thereby increasing the power distributed to the right wheel (Figure 5a) and helping the vehicle quickly overcome the bogged (slippery) region. Similarly, when the left wheel rolls on MD-B, the survey results show that the rotational speeds of both drive axle wheels not only equalize but also reach higher values compared to the MD-A case.

To evaluate the responsiveness of the controller design, Figure 7 presents the velocity deviation between the right and left wheels ($e(t)$) and the brake control torque (M_p). In the initial stage of power increase, the speed deviation rises, the brake control torque increases rapidly, and remains stable to ensure the deviation $e(t)$ stays small (maximum approximately 0.9 rad/s). When the power stabilizes (after 4 seconds), both speed and engine torque decrease, causing $e(t)$ to decline, and the brake control torque decreases accordingly. The greater the adhesion coefficient difference, the higher the brake control torque value.

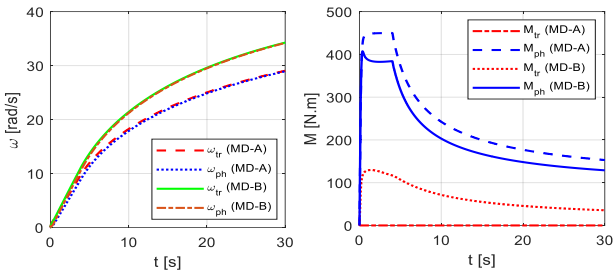

a/ MD-A *b/ MD-B*

Figure 6. *Angular velocity and torque on both sides of the drive wheel*

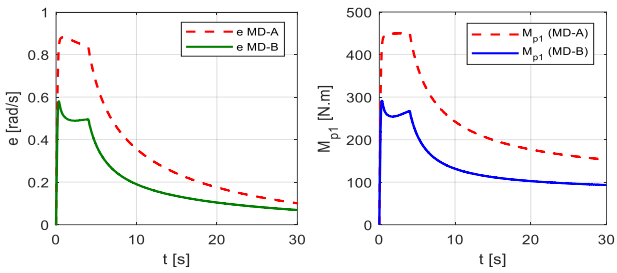

a/ Error angular velocity. *b/ Brake torque*

Figure 7. *Error in angular velocity and brake torque on the left wheel*

The brake torque applied to the brake mechanism, via pulse signals from Controller B, depends on the type of road surface the left wheel traverses. The brake torque value is higher on surfaces with lower adhesion (Figure 7b); initially M_p, it is very large (about 450 [Nm]), but after 4 seconds, it rapidly decreases as the right wheel speed (ω_{ph}) increases and balances with ω_{tr} (Figure 6a).

The achieved results M_p are due to Controller B sending a signal U_S/U_d to the ABS brake actuator, generating brake oil pressure (p_c) in the left wheel brake cylinder according to the pressure calculated by Controller A. The brake oil pressure increases rapidly during the initial stage, then gradually decreases after 4 seconds (Figure 8b). The pressure p_c is lower when the left wheel rolls on a better road surface (MD-B), resulting in a smaller applied brake torque and, consequently, a higher total traction power, enhancing the vehicle's economic efficiency. The pressure deviation (e_p) between the calculated pressure (p_{od}) and the actual pressure in the wheel brake cylinder (p_c) is quite small (Figure 8a), indicating the brake actuator responds well to the designed controller.

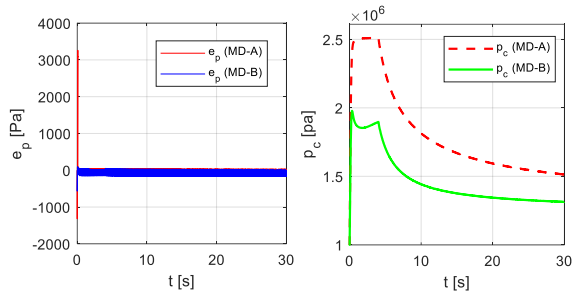

a/ Oil pressure deviation *b/ Wheel cylinder oil pressure*

Figure 8. *Oil pressure deviation in the brake cylinder*

Using the cascade PID controller to regulate the speed of the drive axle wheels and brake oil pressure, which brakes the wheel on the low-adhesion surface with a variable brake torque according to wheel adhesion, enables more uniform distribution of traction power between the two wheels and improves engine power utilization efficiency. Although this solution reduces power loss due to wheel slip, power is still dissipated during braking. The results demonstrate that the cascade controller agreeably distributes traction power at the drive axle wheels, helping the vehicle traverse complex road segments when one wheel is on a slippery surface.

4. Conclusion

This paper presents a method for controlling traction power in automobiles by considering the ABS actuator, through the development of a traction power control model and a hydraulic brake actuator model that accounts for the operation of hydraulic oil valves in the actuator, including models of hydraulic valves and wheel brake mechanisms. The proposed cascade controller is designed to regulate automotive traction power. The controller was tested on two types of road surfaces with different slip conditions, and the survey results show that the designed controller exhibits high responsiveness. Consequently, the traction power transmitted to the left and right wheels on the drive axle varies depending on wheel slip and road surface conditions; the greater the wheel slip, the lower the traction power. The total traction power increases as wheel slip decreases. When one wheel is completely slipping, the total traction power reaches only about 50%, contemporarily, the slip on one wheel is reduced (road type B), and total traction power increases to 62.23%. This demonstrates that traction power is distributed appropriately between the two wheels when using the cascade controller, resulting in more stable vehicle movement, reduced engine power wastage, and improved economic efficiency, especially when driving on poor or complex road surfaces. However, engine power loss occurs during braking control, so brake torque should be considered in controller design.

REFERENCES

[1] K. Han, M. Choi, B. Lee, and S. B. Choi, "Development of a Traction Control System Using a Special Type of Sliding Mode Controller for Hybrid 4WD Vehicles", *IEEE Transactions on Vehicular Technology*, vol. 67, no. 1, pp. 264–274, 2018. DOI: 10.1109/TVT.2017.2752704.

[2] R. He and L. Yuan, "An Improved Nonlinear Predictive Control Strategy Enhanced by Fractional Order Extremum Seeking Control of the Antilock Braking System of a Vehicle", *IEEE Access*, vol. 8, pp. 168576–168588, 2020.

[3] V. T. Trung, N. D. Tuan, and N. H. Vu, "Determination of the tire model coefficient Pacejka of Hyundai Starex car by experiment", *Journal of Science and Technology in Civil Engineering (JSTCE) - HUCE*, vol. 4, no. 11, pp. 101–104, 2017.

[4] J. Fengjiao, L. Zhiyuan, and Z. Hongliang, "A traction control strategy based on optimal slip ratio for the in-wheel motor electric vehicle while steering", in *2015 the 34th Chinese Control Conference*, Hangzhou, China: IEEE, July 2015, pp. 8171–8176.

[5] N. S. An, H. H. Hai, and L. V. Tuan, "Manufacture and operation test of anti-slip braking system on motorcycles", in *Proceedings of the 5th National Conference on Mechanical Science and Technology – VCME 2018*, HaUI, 2018, pp. 800-808.

[6] I. Khan, I. Hussain, M. Z. A. Shah, K. Kazi, and A. A. Patoli, "Design and simulation of anti-lock braking system based on electromagnetic damping phenomena", in *2017 the First International Conference on Latest Trends in Electrical Engineering and Computing Technologies (INTELLECT)*, Karachi, Pakistan: IEEE, Nov. 2017, pp. 1–8.

[7] L. Jin, M. Ling, and J. Li, "Development of a new traction control system using ant colony optimization", *Advances in Mechanical Engineering*, vol. 10, no. 8, pp. 1–12, 2018.

[8] H. Jung, B. Kawak, and Y. Park, "Slip Controller Design for Traction Control System", *International Journal of Automotive Technology*, KSAE, vol. 1, no. 1, pp. 48-55, 2015.

[9] P. Q. Thai, P. V. Binh, and V. C. Tai, "Design of an anti-lock braking control system for motorcycles", *The University of Danang – Journal of Science and Technology,* vol. 18, no. 3, pp. 43-47, 2020.

[10] H. S. Tan and Y. K. Chin, "Vehicle traction control: variable-structure control approach", *Journal of Dynamic Systems Measurement and Control of The American Society of Mechanical Engineers (ASME),* vol. 113, pp. 223-230, 1991.

[11] N. N. Thanh, V. B. K. Trinh, N. V. Nguyen, and T. H. Nhan, "Dynamic analysis of small gasoline car model powertrain using Matlab/Simdriveline", *VNUHCM Journal of Engineering and Technology*, vol. 3, no. SI2, pp. SI176-SI185, 2021.

[12] R. Bengtsson and J. Gundersen, *"Truck Differential and Rear Axle Modeling"*, Master's thesis, Lund University, Sweden, 2010.

[13] G. Liu and L. Q. Jin, "A Study of Coordinated Vehicle Traction Control System Based on Optimal Slip Ratio Algorithm", *Hindawi – Mathematical Problems in Engineering*, vol. 2016, pp. 1–10, 2016.

[14] H.-Z. Li, *et al*., "PID plus fuzzy logic method for torque control in traction control system", *KSAE – International Journal of Automotive Technology*, Vol. 13, No. 3, pp. 441−450, 2012.

[15] S. Saha, H. P. Ikkurti, and S. Saha, "A robust slip-based traction control of electric vehicle under different road conditions", in *Michael Faraday IET International Summit 2015*, Kolkata, India: Institution of Engineering and Technology, 2015, pp. 124–131.

[16] P. T. Tai and T. V. Nhu, "Research control of traction force when an automotive moving on a road with different grip coefficients at the two drive wheels", *Vietnam Mechanical Engineering Journal*, special number 12/2021, pp. 304–309, 2021.

[17] P. T. Tai, T. V. Nhu, and T. Q. Dung, "Using the Brake Torque to Redistribute the Engine Power Transmitting to the Left and Right Drive Wheels", in *Proceedings of the 2nd Annual International Conference on Materials, Machines and Methods for Sustainable Development (MMMS2020),* Vietnam, 2021, pp. 502–507.

[18] C. Jian-wei, C. Liang, C. Wei-feng, and W. Yan-bo, "Modeling and Simulation of ABS Hydraulic Control Unit", in *The 2nd International Conference on Electronic & Mechanical Engineering and Information Technology (EMEIT-2012)*, Jilin University – P. R. China, 2012, pp. 1820-1823.

[19] W. S. Owen, *"An investigation into the reduction of stick-slip friction in hydraulic actuators",* Master's thesis, The University of British Columbia, Canada, 2001.

[20] V. N. Tran, J. Lauber, and M. Dambrine, "Sliding mode control of a dual-clutch during launch", in *The 2nd International Conference on Engineering Mechanics and Automation (ICEMA2),* Hanoi, August 16-17, 2012, pp. 1-10.